International Journal of Engineering, Mathematical and Physical Sciences
ISSN: 2517-9934
Vol:4, No:5, 2010

Evolutionary of prostate cancer stem cells in prostate duct

Zachariah Sinkala

Abstract—A systems approach model for prostate cancer in prostate duct, as a sub-system of the organism is developed. It is accomplished in two steps. First this research work starts with a nonlinear system of coupled Fokker-Plank equations which models continuous process of the system like motion of cells. Then extended to PDEs that include discontinuous processes like cell mutations, proliferation and deaths. The discontinuous processes is modeled by using intensity poisson processes. The model incorporates the features of the prostate duct. The system of PDEs spatial coordinate is along the proximal distal axis. Its parameters depend on features of the prostate duct. The movement of cells is biased towards distal region and mutations of prostate cancer cells is localized in the proximal region. Numerical solutions of the full system of equations are provided, and are exhibit traveling wave fronts phenomena. This motivates the use of the standard transformation to derive a canonically related system of ODEs for traveling wave solutions. The results obtained show persistence of prostate cancer by showing that the non-negative cone for the traveling wave system is time invariant. The traveling waves have a unique global attractor is proved also. Biologically, the global attractor verifies that evolution of prostate cancer stem cells exhibit the avascular tumor growth. These numerical solutions show that altering prostate stem cell movement or mutation of prostate cancer cells lead to avascular tumor. Conclusion with comments on clinical implications of the model is discussed.

Keywords—Fokker-Plank equations, global attractor, stem cell.

I. Introduction

Prostate cancer is an evolutionary process involving natural selection among prostate cancer stem cells [19]. The selection of prostate cancer is driven typically by differential replication of cells that differ phenologically as a result of genetic mutations of prostate stem cell. The organism responses represents the immune system attack on cells recognized as foreign which has really been demonstrated as crucial to early stages of natural prostate cancer suppression [22], [11]. Predation of the immune system selects variants that are less immunogenic [12]. A sub population of prostate cancer stem cells might escape by evading the immune system [23].

There are three main phases of solid tumor cancer: avascular,vascular and metastatic [17], [33]. The prostate gland contains a branched network of ducts which directs seminal fluid toward the urethra [46]. The lumen of the ducts is lined by the prostate epithelium, which is composed of two cell layers Figure 1. b : an underlying basal layer that is discontinuous comprising stem cells and intermediate transit amplifying cells(TA/IC) and an overlying luminal layer containing luminal cells responsible for producing seminal fluid and secreting it into the lumen [49]. The longitudinal axis of a prostate duct

Z. Sinkala is with the Department of Mathematical Sciences, Middle Tennessee State University, Murfreesboro, TN, 37132 USA e-mail: zsinkala@mtsu.edu.

Manuscript received March 23, 2010; revised March 23, 2010.

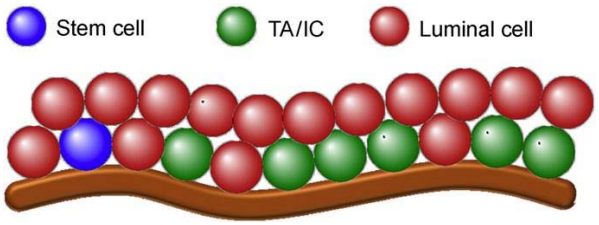

Fig. 1. b :Illustration of a healthy the basal and luminal layers of the prostate epithelium.

is divided into three regions which are classified according to their distance from the urethra: The proximal, intermediate, and distal regions [28], [35], [38]. The proximal region of the prostatic ducts harbor the prostatic epithelial stem cells [49]. It would seem that stem cells in the basal layer in proximal region give rise to progeny consisting of TA/IC cells, which in turn differentiate into the functional, secretory luminal cells [30], [7], [47]. Homeostasis of the prostate epithelium is maintained by prostatic adult stem cells, which are localized in the proximal region and proliferate to give rise to the cells that populate the epithelium . The proliferation rate of epithelial cells is balanced by an equal rate of cell death, so that no net change in total epithelial cell number occurs. To achieve this balance, the stem cell proliferation rate must be tightly controlled. At least part of this control is achieved through transforming growth factor-β (TGF-β), which is an extracellular factor secreted by prostate epithelial cells and by the stromal cells which support the prostate epithelium. TGF-β inhibits cellular proliferation when administered to prostate epithelial cells.

Most evidence suggest the relevance of a preliminary model that focuses on mutant basal stem cells as the primary source of cancer cell lines. Prostate cancer basal stem cells move to intermediate or distal to proliferate. Specifically, a model whereby mutant stem cells lead to mutant progeny, and consequently to the burgeoning of (heterogeneous) tumor growth is developed. In the model, prostatic stem cells, cancer prostatic stem cells and progeny prostatic cancer stem cells were explicitly represented in a one-dimensional reconstruction of a prostate duct along proximal-distal axis. Following standard methodology, the purpose of the model in this work is toward identifying the dynamics of some of the key elements operative in the progression of the avascular stage of prostate tumor development. The model does not distinguish types of mutant progeny cells, but look to overall net progeny $\tilde{P}$ of net mutant stem cells $\tilde{S}$, and net densities of healthy prostatic stem cells S. "Defective cells would mark the transition between pre-

tumor to tumor progression" [9]. The mutant progeny term $\tilde{P}$ is therefore the amalgamation of all types of tumorous cells, excluding the mutant basal stem cell population $\tilde{S}$. There is evidence that prostate stem cell movement can dysregulate epithelial homeostasis and lead to excessive cell growth, suggesting that disruption of cell movement may contribute to prostate cancer [27]. There is evidence that there is two possible ways of causes of prostate cancer: (i) Mutant stem cells and (ii) Altering prostate stem cells movement. The mutant stem cell approach has advantages over the second approach for the following reasons: (i) This research focus in results that are easily clinically verifiable. Thus the first approach is favored. The second approach has no vivo experiments to compute the parameters for modeling but some vitro experiment have done to support the hypothesis [27] . The net population $\tilde{P}$ would correspond with overall tumor density - a quantity that is relatively accessible; (ii) The results in this work suggest that the present model provides clinically plausible population profiles; and (iii) The basic structure of the model can naturally accommodate additional elements, cell types, etc., as needed. In future work, therefore, the plan is to include heterogeneity of cells, additional biochemical and cellular network interactions, as well as treatment terms.

In the literature, there already are ODE (ordinary differential equations) models that include stem cell population densities, for example [14], [10]. The Ganguly et al. [14] model quantifies generations of progeny of a single cell line, rather than heterogeneous cell lines as such. The model includes self-renewal rates of the cell population compartments, corresponding to clinical evidence that in some cases, daughter cells can belong to the compartment of origin. In fact daughter cells can also belong to earlier compartments in a cell line [29]. Clinical techniques presently available, however, do not allow for easy identification *in vivo* of the generation to which a cell belongs (relative to a source). Consequently, the self-renewal rates in the model of [14] are not at this time directly clinically verifiable. In order to meet requirement (i) above it is important to ignore internal fluctuations in cell lines, and look instead to net population quantities.

In [10], [14], [32], [45], [48], one finds quantitative results based on numerical simulations. These numerical results invite further theoretic development. As this work show, precise stability analysis can provide boundary conditions which could have clinical implications.

Another feature of the models of [10], [14] and others is that cancer cell populations are modeled in isolation, that is, as independent growth processes. If one tracks the population growths through the models in [10] and [14], one obtains exponential growth of initial population densities. This, however, is not realistic *in vivo*, except perhaps for the most initial time period of positive net mutation, or for cancer growth *in vitro*. Cancer as such, occurs *in vivo* and afflicts an organism. An organism typically responds to mutation by employing various corrective measures. Even in a healthy organism, mutations occur on a regular basis, but unhealthy cells are destroyed or flushed from the system. An organism becomes diseased when mutation types and rates exceed the response capacity of the organism [2]. In [44]looked at mutant stem cell approach. They used a PDE with one dimensional spatial coordinates to model. In their model the spatial coordinates did not fully address the prostate duct features. For example that the stem cells are primarily located in the proximal region. All parameters used in their model were constant and they did not incorporate features of the prostate duct. The specifics of organism response can of course be extremely complex, involving an orchestrated panoply of system-wide biochemical and cellular processes. For now, the plausibility of the approach in this work is investigated, by looking to the overall effect of a generic response term. Analysis of specific corrective processes (T - cells, etc) to future work is deferred. As is well known, cells have contact dynamics ["contact inhibition (and lack) of migration" [1]].

They therefore also include diffusion terms to model spatial extension of tumor growth. This work model consists of a system of coupled PDEs (partial differential equations) to model the spatial spread of tumor growth resulting from contact dynamics, spatial diffusion and biased cell motion toward the distal region. In this work, it is assumed that stem cells reside in proximal region and are assumed stationary [27]. The advection term is included since the prostate cancer cells to proliferate have to move to distal region [27]

As described above, their model focuses on a mutant stem cell population that leads to mutant progeny, and consequently to the burgeoning of (heterogeneous) tumor growth [30], [47], [7], [40]. Therefore three cell populations are obtained, namely, healthy stem cells, mutant stem cells and progeny of mutant stem cells. The PDE involving stem cells evolution does not have the diffusion term since prostate stem cells are stationary in the proximal region. Quinn and Sinkala [44] introduction of second order partial derivatives was partly motivated by the work of [4] on two interacting populations that disperse to avoid crowding. The model in this work, though, includes three populations. One also draw from the work of [1] on contact inhibition (and lack) of migration and biased cell motion toward distal region. Putting these results together produces a model that includes a system of coupled Fooker-Planck equations. Then the poisson process terms included to a system of Fokker-Planck equation type. The mathematical analysis is partly motivated by the work of [42] on avascular tumor growth. In [42], the three cell populations modeled are proliferating, quiescent and necrotic cells. The model in this work is for stem cells, mutant stem cells, and progeny of mutant stem cells. A key features of our model is inclusion of features of prostate duct in the terms of the PDEs, biased motion of cells, parameters depends on spatisal proximal-distal coordinate and prostate stem cells are stationary. It is not intended that the source is independent as such. Within the whole organism one of the basic tenets of the system approach is that the production of all cell types (in particular basal stem cells, mutant stem cells and progeny) depends on the whole organism. It follows that within the prostate, organism response terms can be included as non-constant functions of several variables, defined by locally interacting quantities and by the whole organism response.

There are new clinical results that seem to support the need for the development of models that include organism response

terms and parameters depending on proximal-distal coordinate. Indeed, there has been a promising build up of results toward the possibility of treating certain cancers by using non-toxic drugs that activate and/or assist the immune system response through specific molecular markers. With regard to prostate cancer, see [18], [6], [37], [21], [25], [50]. For prostate cancer James P. Allison and his team - see [39] found evidence that immune system can recognize prostate cancer stem cells. The response of the immune system was feeble [31]. See also [12]. The literature is, in fact, rich in cancer research that investigates the role of the immune system. As pointed out in [**?**], it is increasingly feasible that this accumulation of results involving organism response means that in the future, ranges of clinically useful models will significantly benefit from the inclusion of organism and/or immune response terms and features of prostate duct. In particular, a clinically useful expansion of test model in this work might therefore include reaction pathway structures in the human organism.

More work would be needed to make their test model directly clinically applicable. At this time, however, the necessary laboratory quantities and parameters are not yet available. However, there would seem to be grounds for further development of models that include organism response terms and biased motion terms. In model in this work, inclusion of an organism response term suppresses tumor growth, while exclusion of the response term leads to eradication of basal cell populations. This article is demonstrated both theoretically and computationally. Indeed, inclusion of the response term in our model is what leads to the existence of a global attractor with strictly positive cell densities. In other words, our results are also consistent with clinical results corresponding to the relatively stable avascular stage of tumor growth. Note too that our results are consistent with the recently published laboratory results of Allison et al, referenced above. In other words, it is now known that organism response can play an effective role in limiting cancer growth.

For the model in this work one include alteration of stem cells or mutant stem cells with organism response. The PDE will have diffusion terms and advection terms.

The paper is structured as follows: Following Section 1 Introduction. Section 2 Construction of the model; Section 3 Rescaling the system of PDEs; Section 4 Analytic approximation; Section 5 Persistence. We use technique similar to Quinn and Sinkala [44] Section 6 Stability analysis for persistence; Section 7 Clinical implications; Section 8 Conclusion.

II. Building of the Model

For the model in this work, one let the populations defined by

$$S = \text{basal stem cells} \tag{1}$$

$$\widetilde{S} = \text{mutant basal stem cells} \tag{2}$$

$$\widetilde{P} = \text{progeny of mutant basal stem cells} \tag{3}$$

One assume that the total basal cell population $B(t) = S(t) + \widetilde{S}(t)$ is constant. Consequently, $B = B(0)$ is the carrying capacity for the total number of all basal stem cells, both healthy and mutant. $\mu_i(x), i = 0, 1$ represent mutation terms see the flow chart given in Figure 6. where

$$\mu_i(x) = \begin{cases} \mu_i \text{ if } 0 \leq x \leq \text{length of duct}/3 \\ 0 \text{ otherwise} \end{cases} \tag{4}$$

and

$$\alpha_1(x) = \begin{cases} \alpha_1 \text{ if } 0 \leq x \leq \text{length of duct}/3 \\ 0 \text{ otherwise} \end{cases} \tag{5}$$

These parameters depends on spatial coordinate along proximal -distal axis. The response term parameter is represented by R_0 are assumed to be scalar functions depending on net mutations.

Note the flow chart given in Figure 6, for stem cells, mutant stem cells and progeny of mutant stem cells in prostate duct. This structure implies the following: (i) Since for this system there is no population in the model that is prior to healthy basal stem cells, there is consequently no IN term coefficient μ_{-1} ; (ii) The constant $\mu_0(x)$ stands for the mutation rate of healthy stem cells into mutant stem cells; (iii) The constant $\mu_1(x)$ stands for the production rate of mutant stem cells into progeny of mutant stem cells; and (iv) The constant μ_2 stands for the natural death rate of mutant progeny. For the avascular stage of tumor growth, we assume that $\mu_2 = 0$.

In the next section, one indicate provisional values for constants corresponding to each of the cell types. Note that we were not able to find an abundance of clinical data in the literature. See however Table 1 and [10], [14], [36], [48].

It is known that stem cell populations are maintained over the lifetime of the organism. "(It) is generally accepted that cancer development occupies a significant time-span in humans. In many tissues, the restricted progenitors and differentiated cells tend to have a (relatively) short life-span" [7]. This is "(in) contrast to the stem cells, which persist throughout life in (these) tissues" [7]. Since the architecture of the prostate [7] is maintained throughout the avascular stage of prostate cancer, one make the approximating assumption that the total number of basal stem cells (healthy plus mutant) remains constant and basal stem cells are located in the proximal region of the prostate duct. One also assume that basal stem cells are stationary in the the proximal region. In other words, while mutations of healthy stem cells slowly reduce the concentrations of healthy stem cells S, and such mutations then contribute to the mutant stem cell concentrations $\tilde{S}$. The maintenance of the prostate architecture leads us to the approximation $B = S + \tilde{S}$ for some constant B.

Again, since the architecture of the gland is maintained, one assume that the net primary growth rate of healthy basal stem cells is zero. This implies that $\alpha_0 = 0$.

As described in the Introduction, one of the basic tenets of the system and sub-system approach is that the production of all cell types (in particular basal stem cells, mutant stem cells and progeny) depends on the complex, flexible, but directed functioning of the whole organism. It follows that locally (within the prostate) organism response terms can be included as non-constant functions of several variables, driven both by locally interacting quantities and by the whole organism response. As basal stem cells mutate, the prostate

loses its natural source of healthy stem cells. For the organism response, one assume that the response rate is proportional to both the mutation rate $\mu_0(x)$ and $\frac{\tilde{S}}{B}$ (the relative build up of mutant stem cells $\tilde{S}$ compared to the carrying capacity B of all stem cells). One therefore take the organism response term to be $R_0 = \frac{\rho\mu_0}{B}\tilde{S}$, for some $\rho \in [0,1]$.

Since, the mutant basal stem cell population is of low density (Collins et al., 2006), as an approximation one assumes that the organism response to this low density flux in stem cell character is negligible. One therefore take $R_1 = 0$.

Compared to healthy cells, mutant stem cells and their progeny significantly differ in their growth rate signatures. For the growth rate of the avascular tumor (progeny of mutant basal stem cells , one take $\alpha_2 = 0.09$. See Table I and [48]. For the net growth rate of mutant basal stem cell concentrations, one uses $\alpha_1 = 0.01$ in Equation (5). See Table I and [10]. Despite relative low density of mutant stem cells, being mutant means that growth rates may depend somewhat on interaction with other mutant stem cells. One uses $\alpha_{11} = 0.01$. See Table I and [10]. For interaction of progeny with progeny one takes $\alpha_{22} = .01$. See Table I and [48]. Lacking further clinical data at this time, one assumes that the interaction between progeny of mutant stem cells may require $\alpha_{21} > 0$.

For the avascular phase, there is a build up of tumor growth that is of relatively modest dimensions within the epithelial tissue [7]. Moreover, at this stage, cancerous growth would seem to make effective use of available resources, without effective direct response from the organism. [See, however, [39], results of which will need to be eventually included in a more complete model.] As a first approximation one therefore assumes that the organism response to the progeny is given by $R_2 = 0$.

Cell densities are functions of both location x and time t . One write $S(x,t)$; $\widetilde{S}(x,t)$; and $\widetilde{P}(x,t)$. The spatial variable x is taken to be one-dimensional and is along proximal-distal axis. The variable x therefore corresponds to an average radial growth distance of the tumor away from the initial center. One hypothesizes that this idealization is reasonable as an approximation, since in the avascular phase early formation of tumors is confined to epithelium cells.

One build the model similar approach taken by Quinn and Sinkala [44] but in this work case one do include the features of the prostate duct. One obtain the a system of PDEs for $S(x,t)$, $\widetilde{S}(x,t)$ and $\widetilde{P}(x,t)$. One also assume that cell movement is biased and directed from proximal to distal region and stem cells are stationary. The unbiased movement is modeled by Fokker-Planck diffusion. One therefore obtain

$$\frac{\partial S}{\partial t} = -\mu_0(x)S + \frac{\rho\mu_0(x)}{B}\widetilde{S} \tag{6}$$

$$\begin{aligned}&\tfrac{\partial \widetilde{S}}{\partial t} = \tfrac{\partial}{\partial x}\left(\tfrac{\widetilde{S}}{\widetilde{S}+\widetilde{P}}\tfrac{\partial(\widetilde{S}+\widetilde{P})}{\partial x}\right)\\ &+\alpha_1(x)\widetilde{S} - v_0\tfrac{\partial \widetilde{S}}{\partial x} - \tfrac{1}{B}\alpha_{11}\widetilde{S}^2 - \mu_1(x)\widetilde{S} + \mu_0 S\end{aligned} \tag{7}$$

$$\frac{\partial \widetilde{P}}{\partial t} = \frac{\partial}{\partial x}\left(\frac{\widetilde{P}}{\widetilde{S}+\widetilde{P}}\frac{\partial(\widetilde{S}+\widetilde{P})}{\partial x}\right) + \alpha_2\widetilde{P} - \frac{1}{B}\alpha_{22}\widetilde{P}^2 + \mu_1(x)\widetilde{S} \tag{8}$$

where v_0 is the velocity of prostate cancer stem cells is approximately 3μ meters per hour.

III. Re-scaling the system of partial differential equations

For convenience, one rescales the system of partial differential equations (6)-(8) [43]. We substitute; $\bar{t} = t\alpha_2$, divide the first and second equations by α_2(is assumed constant), and then set $\bar{x} = x\sqrt{\alpha_2}$. This yields

$$\frac{\partial S}{\partial \bar{t}} = -\frac{\mu_0(x)}{\alpha_2}S + \frac{\rho\mu_0(x)}{B\alpha_2}\widetilde{S} \tag{9}$$

$$\begin{aligned}&\tfrac{\partial \widetilde{S}}{\partial \bar{t}} = \tfrac{\partial}{\partial \bar{x}}\left(\tfrac{\widetilde{S}}{\widetilde{S}+\widetilde{P}}\tfrac{\partial(\widetilde{S}+\widetilde{P})}{\partial \bar{x}}\right)\\ &-\tfrac{v_0}{\alpha_2}\tfrac{\partial \widetilde{S}}{\partial \bar{x}} + (\tfrac{\alpha_1}{\alpha_2} - \tfrac{\mu_1}{\alpha_2})\widetilde{S} - \tfrac{1}{B\alpha_2}\alpha_{11}\widetilde{S}^2 + \tfrac{\mu_0(x)}{\alpha_2}S\end{aligned} \tag{10}$$

$$\frac{\partial \widetilde{P}}{\partial \bar{t}} = \frac{\partial}{\partial \bar{x}}\left(\frac{\widetilde{P}}{\widetilde{S}+\widetilde{P}}\frac{\partial(\widetilde{S}+\widetilde{P})}{\partial \bar{x}}\right) + \widetilde{P} - \frac{1}{B\alpha_2}\alpha_{22}\widetilde{P}^2 + \frac{\mu_1(x)}{\alpha_2}\widetilde{S} \tag{11}$$

Numerical simulations of the full system of PDEs (9-11) are given in figures 3,4 and 5. For each cell density $S, \widetilde{S},$ and $\widetilde{P}$ one sees that time evolution produces an advancing pulse, or wave front. This motivates the strategy of Section 4. (Note that clinically verified parameters can be difficult to find. One used the values listed in Table 1, obtained from the literature search in [44].)

IV. Analytic approximation

The goal in this section is to obtain solutions that approximate the wave-front behavior exhibited in the numerical solutions in Figures 3, 4 and 5. One therefore uses a well known canonical transformation of coordinates for obtaining possible solutions of the traveling wave form

$$S(\bar{x},\bar{t}) = s(z),\ \widetilde{S}(\bar{x},\bar{t}) = \widetilde{s}(z),\ \widetilde{P}(\bar{x},\bar{t}) = \widetilde{p}(z),\ z = \bar{x} - v\bar{t}, \tag{12}$$

where v is the wave speed.

Substitution of these solution forms transforms the PDEs (9-11) into the ODEs

$$\begin{aligned}&vs' - \tfrac{\mu_0}{\alpha_2}s + \tfrac{\rho\mu_0}{B\alpha_2}\widetilde{s} = 0\\ &(v+v_0)\widetilde{s}' + \left(\tfrac{\widetilde{s}(s'+\widetilde{s}'+\widetilde{p}')}{s+\widetilde{s}+\widetilde{p}}\right)'\\ &+\tfrac{\alpha_1}{\alpha_2}\widetilde{s} - \tfrac{1}{B\alpha_2}\alpha_{11}\widetilde{s}^2 - \tfrac{\mu_1}{\alpha_2}\widetilde{s} + \tfrac{\mu_0}{\alpha_2}s = 0\\ &v\widetilde{p}' + \left(\tfrac{\widetilde{p}(s'+\widetilde{s}'+\widetilde{p}')}{s+\widetilde{s}+\widetilde{p}}\right)' + \widetilde{p} - \tfrac{1}{B\alpha_2}\alpha_{22}\widetilde{p}^2 + \tfrac{\mu_1}{\alpha_2}\widetilde{s} = 0\end{aligned} \tag{13}$$

TABLE I
PARAMETERS DATA OF EQUATIONS (6-8)

$\rho \in [0,1]$	organism response rate
$B = 1$	carrying capacity of all stem cells, healthy and mutant together
$\alpha_1 = .01$	growth rate of mutant basal stem cells [10]
$\alpha_{11} = .01$	logistic constant for mutant stem cells (MSC) [48]
$10^{-7} \leq \mu_0 \leq 10^{-2}$	rate constant for healthy stem cells to mutant stem [14],
$\mu_1 = .00995$	differentiation rate constant for the MSC to progeny number [36]
$\alpha_2 = .09$	growth rate of progeny of MSC [48]
$\alpha_{22} = .01$	logistic constant for progeny of mutant stem cells [48]

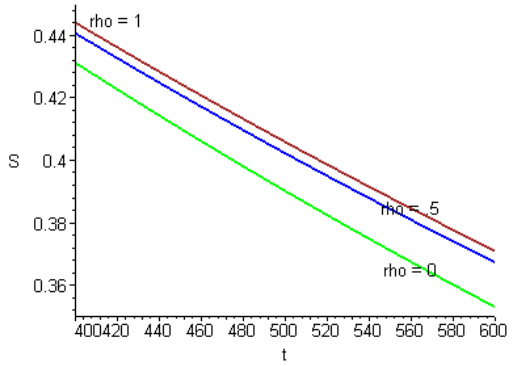

Fig. 2. Numerical solutions of the model (6-8). In this figure we represent a window of three different dynamics of stem cell densities (denoted by S) at three different organism responses, namely, organism response, $\rho = 0, 0.5,$ and 1. These densities are plotted as functions of time at $x = 0$. The initial conditions were $\tilde{S} = 0, \tilde{P} = 0, S = \exp(-0.1x)$. The figure demonstrates that the increased stem cell density as a function of organism response just like observed in [44].

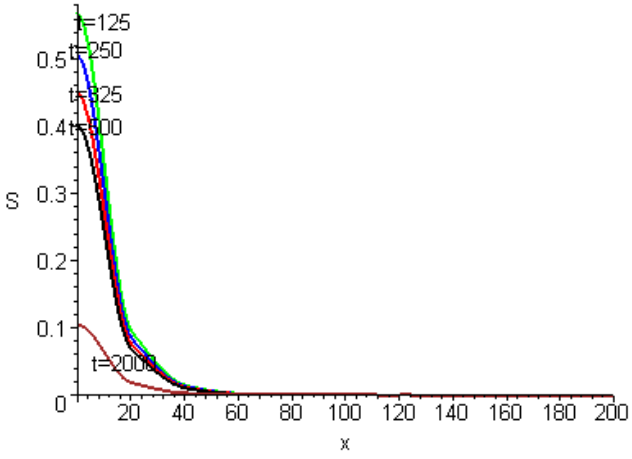

Fig. 3. Numerical solutions of the model (6-8). In this graph the symbol S represents stem cell densities. These are plotted as functions of space at times $t = 125, 250, 375, 500, 2000$. The initial conditions were $\tilde{S} = 0, \tilde{P} = 0, S = \exp(-0.1x)$, organism response, $\rho = 0.5$ and the boundary conditions used were $\frac{\partial S}{\partial x} = \frac{\partial \tilde{S}}{\partial x} = \frac{\partial \tilde{P}}{\partial x} = 0$. x coordinate is along proximal-distal axis with scale unit x-coordinate represents $\frac{1}{80}$ of the prostate duct.

A. Approximating the Minimum Speed.

In the model in this work, cell growth is centered about $(s = 0, \tilde{s} = 0, p = 0)$. The pair $s = 0$, $\tilde{s} = 0$ determines the center for a Taylor expansion. The allowed values for s and $\tilde{s}$ are then non-negative with $s + \tilde{s} = B > 0$. [This technique allows for analysis of population dynamics near a steady state. See also [43], [15]. By the classical theory of ODE's one therefore looks for solutions of the form

$$s(z) = \widehat{s}\exp(-\xi z),\ \widetilde{s}(z) = \widehat{\widetilde{s}}\exp(-\xi z),\ \widetilde{p}(z) = \widehat{\widetilde{p}}\exp(-\xi z).$$

Since cancer does not usually behave periodically, one also requires that ξ be real(Imaginary part $\xi = 0$). Substituting into (13) and taking only leading order terms gives

$$-v\xi\widehat{s} + \xi^2\widehat{s} - \frac{\mu_0}{\alpha_2}\widehat{s} + \frac{\rho\mu_0}{B\alpha_2}\widehat{\widetilde{s}} = 0 \tag{14}$$

$$-(v_0 + v)\xi\widehat{\widetilde{s}} + \xi^2\widehat{\widetilde{s}} + \frac{\alpha_1}{\alpha_2}\widehat{\widetilde{s}} - \frac{\mu_1}{\alpha_2}\widehat{\widetilde{s}} + \frac{\mu_0}{\alpha_2}\widehat{s} = 0 \tag{15}$$

$$-v\xi\widehat{\widetilde{p}} + \xi^2\widehat{\widetilde{p}} + \widehat{\widetilde{p}} + \frac{\mu_1}{\alpha_2}\widehat{\widetilde{s}} = 0 \tag{16}$$

Thus for nontrivial solutions, we must have

$$\xi(x) = \frac{1}{2}\left[v \pm \sqrt{v^2 - 4\left(1 + \frac{\mu_1(x)}{\alpha_2}\frac{\widehat{\widetilde{s}}}{\widehat{\widetilde{p}}}\right)}\right] \tag{17}$$

The existence of a minimum wave speed is similar to the result for the reaction-diffusion equation studied by Fisher (1937). It is known that a wave moving with minimum speed evolves from sufficiently localized data. One therefore anticipates that the speed of the tumor growth implied by equations (9 - 11) will be bounded below by 2. One notes that while clinical verification remains to be obtained, this is confirmed in numerical simulations.

B. Rescaling the traveling wave equation.

To obtain a stability analysis of (13), one modifies a method developed by Canosa [5] for approximation of the Fisher equation. This involves rescaling the traveling wave coordinate by writing $\zeta = -z/v$ and leads to the equivalent system

$$\begin{aligned}
&-\tfrac{ds}{d\zeta} - \tfrac{\mu_0}{\alpha_2}s + \tfrac{\rho\mu_0}{B\alpha_2}\widetilde{s} = 0\\
&-(1 + \tfrac{v_0}{v})\tfrac{d\widetilde{s}}{d\zeta} + \tfrac{1}{v^2}\tfrac{d}{d\zeta}\left(\tfrac{\widetilde{s}}{s+\widetilde{s}+\widetilde{p}}\tfrac{d(s+\widetilde{s}+\widetilde{p})}{d\zeta}\right)\\
&+\tfrac{\alpha_1}{\alpha_2}\widetilde{s} - \tfrac{1}{B\alpha_2}\alpha_{11}\widetilde{s}^2 - \tfrac{\mu_1}{\alpha_2}\widetilde{s} + \tfrac{\mu_0}{\alpha_2}s = 0\\
&-\tfrac{d\widetilde{p}}{d\zeta} + \tfrac{1}{v^2}\tfrac{d}{d\zeta}\left(\tfrac{\widetilde{p}}{s+\widetilde{s}+\widetilde{p}}\tfrac{d(s+\widetilde{s}+\widetilde{p})}{d\zeta}\right) + \widetilde{p} - \tfrac{1}{B\alpha_2}\alpha_{22}\widetilde{p}^2 + \tfrac{\mu_1}{\alpha_2}\widetilde{s} = 0
\end{aligned} \tag{18}$$

Under present biological hypothesis and as in Sheratt and Chaplain [43], one obtains the reduced equation

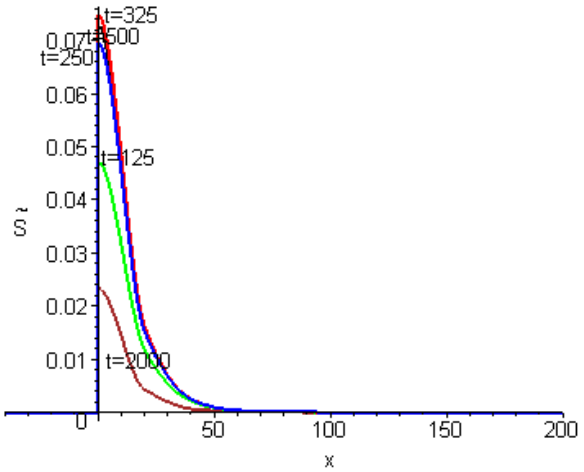

Fig. 4. Numerical solutions of the model (6-8). In this graph the symbol $\tilde{S}$ represents cancer stem cell densities. These are plotted as function of space at times $t = 125, 250, 375, 500, 3000$. The initial conditions were $\tilde{S} = 0, \tilde{P} = 0, S = \exp(-0.1x)$, organism response, $\rho = 0.5$, and the boundary conditions used were $\frac{\partial S}{\partial x} = \frac{\partial \tilde{S}}{\partial x} = \frac{\partial \tilde{P}}{\partial x} = 0$. x coordinate is along proximal-distal axis with scale unit x-coordinate represents $\frac{1}{80}$ of the prostate duct.

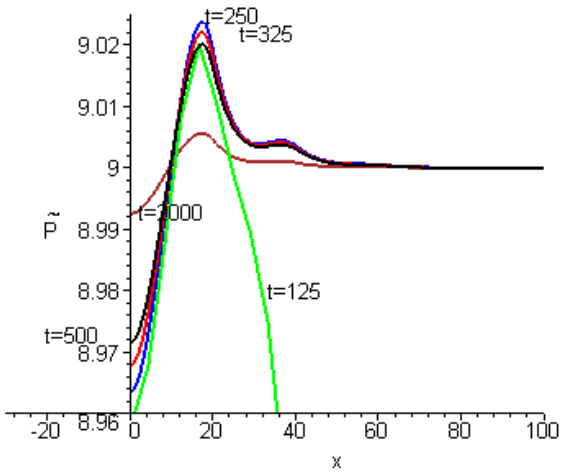

Fig. 5. Numerical solutions of the model (6-8). In this graph the symbol $\tilde{P}$ represents cancerous progeny cell densities. These are plotted as functions of space at times $t = 125, 250, 375, 500, 2000$. The initial conditions were $\tilde{S} = 0, \tilde{P} = 0, S = \exp(-0.1x)$, organism response, $\rho = 0.5$ and the boundary conditions used were $\frac{\partial S}{\partial x} = \frac{\partial \tilde{S}}{\partial x} = \frac{\partial \tilde{P}}{\partial x} = 0$. x coordinate is along proximal-distal axis with scale unit x-coordinate represents $\frac{1}{80}$ of the prostate duct.

$$\begin{aligned} &-\tfrac{ds}{d\zeta} - \tfrac{\mu_0}{\alpha_2} s + \tfrac{\rho\mu_0}{B\alpha_2}\widetilde{s} = 0 \\ &-(1+\tfrac{v_0}{v})\tfrac{d\widetilde{s}}{d\zeta} + \tfrac{\alpha_1}{\alpha_2}\widetilde{s} - \tfrac{1}{B\alpha_2}\alpha_{11}\widetilde{s}^2 - \tfrac{\mu_1}{\alpha_2}\widetilde{s} + \tfrac{\mu_0}{\alpha_2} s = 0 \\ &-\tfrac{d\widetilde{p}}{d\zeta} + \widetilde{p} - \tfrac{1}{B\alpha_2}\alpha_{22}\widetilde{p}^2 + \tfrac{\mu_1}{\alpha_2}\widetilde{s} = 0 \end{aligned} \tag{19}$$

Let

$$u = \frac{1}{1+\frac{v_0}{v}}, v > 0.$$

V. Persistence

In order for a model to be biologically feasible, it is normally required that "persistence" be established. See, e.g., [34], [16], and [20]. For our model this means that we need to prove that the non-negative cone $\mathcal{C} = \{(s, \tilde{s}, \tilde{p}) \mid s \geq 0,\ s \geq 0,\ \tilde{p} \geq 0\}$ is invariant with respect to scaled time ζ. Recall that in geometric terms, the trajectories of an ODE

$$\left(\frac{ds}{d\zeta}, \frac{d\tilde{s}}{d\zeta}, \frac{d\tilde{p}}{d\zeta}\right) = \mathbf{v}\left(s, \tilde{s}, \tilde{p}\right)$$

are the integral curves of the defining vector field

$$\mathbf{v}\left(s, \tilde{s}, \tilde{p}\right) = \left(\mathbf{v}_1, \mathbf{v}_2, \mathbf{v}_3\right)$$

where

$$\mathbf{v}_1 = -\frac{\mu_0}{\alpha_2} s + \frac{\rho\mu_0}{B\alpha_2}\widetilde{s},$$

$$\mathbf{v}_2 = u\left(\frac{\mu_0}{\alpha_2} s + (\frac{\alpha_1}{\alpha_2} - \frac{\mu_1}{\alpha_2})\widetilde{s} - \frac{\alpha_{11}}{B\alpha_2}\widetilde{s}^2\right),$$

$$\mathbf{v}_3 = \frac{\mu_1}{\alpha_2}\widetilde{s} + \widetilde{p} - \frac{\alpha_{22}}{B\alpha_2}\widetilde{p}^2.$$

One therefore examines the behavior of this vector field along the boundaries of the non-negative cone $\mathcal{C}$.

For convenience, one makes the following identifications:

$$a = \frac{\mu_0}{\alpha_2},\ b = \frac{\rho\mu_0}{B\alpha_2},\ c = \frac{\alpha_1}{\alpha_2},\ d = \frac{\alpha_{11}}{B\alpha_2},\ e = \frac{\mu_1}{\alpha_2},\ f = \frac{\alpha_{22}}{B\alpha_2}.$$

The vector field becomes

$$\mathbf{v}\left(s, \tilde{s}, \tilde{p}\right) = \left(-as + b\widetilde{s}, u(as + (c-e)\widetilde{s} - d\widetilde{s}^2), e\widetilde{s} + \widetilde{p} - f\widetilde{p}^2\right).$$

The boundary of the non-negative cone is determined by the coordinate planes: I denotes the $(\widetilde{p} = 0)/(s, \widetilde{s})$ plane; II denotes the $(s = 0)/(\tilde{s}, \widetilde{p})$ plane; and III denotes the $(\tilde{s} = 0)/(s, \widetilde{p})$ coordinate plane. All three planes intersect in the origin; each pair of planes intersect in one of the non-negative coordinate lines; and each plane has its own relative interior. One analyzes each of these sets in turn. Note that $\cap$ denotes set-theoretic intersection.

$I \cap II \cap III$: The origin is clearly an equilibrium point for the vector field.

$I \cap III$: Along the strictly positive $s > 0$ - axis, $\mathbf{v}\left(s, \tilde{s}, \tilde{p}\right) = (-as, uas, 0)$. This generator points along the coordinate plane II.

$I \cap II$: Along the strictly positive $\tilde{s} > 0$ - axis,

$$\mathbf{v}\left(s, \tilde{s}, \tilde{p}\right) = \left(b\widetilde{s}, u\left((c-e)\widetilde{s} - d\widetilde{s}^2\right), e\widetilde{s}\right).$$

It follows that along the $\tilde{s} > 0$ - axis, the vector field points toward the interior of the cone.

Regarding the second coordinate of the vector field, note that

$$c - e = \frac{\alpha_1 - \mu_1}{\alpha_2}. \tag{20}$$

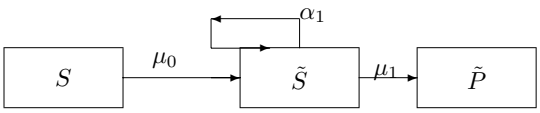

Fig. 6. A schematic diagram of $\tilde{S}$ compartment. μ_0, α_1, μ_1 depend on spatial coordinate x along proximal-distal axis of the prostate duct.

Figure 6 shows three rate constants that govern the population of the $\tilde{S}$ compartment, namely, α_1, μ_0, μ_1. If the disease is progressive, $\tilde{s}$ is assumed to be increasing, and so one takes $\alpha_1 + \mu_0 > \mu_1$. But, μ_0 corresponds to a relatively rare event [32], hence α_1 is the dominant term of the left-hand side of this inequality. For our model, we therefore assume that $\alpha_1 > \mu_1$, from which it follows that $c - e > 0$. Note that this is consistent with clinical data recorded in Table I.

It follows that the second coordinate has a zero along this axis. At that point, the vector field is parallel to the s - plane, but still points to the interior of the non-negative cone $\mathcal{C}$.

$II \cap III$: Along the strictly positive $\tilde{p} > 0$ axis, the vector field is $\mathbf{v}(s, \tilde{s}, \tilde{p}) = \left(0, 0, \widetilde{p} - f\widetilde{p}^2\right)$. Initial values near the origin flow the along $\tilde{p}$ axis toward fixed point $(0, 0, 1/f)$. Beyond the fixed point, the flow reverses and is directed back toward the fixed point.

Next, one looks to the interiors of the three coordinate planes. For simplicity of notation, one uses I, II, III to indicate each case, where it is understood that one is looking to interior points of each plane (relative topology).

$$I: \ (\widetilde{p} = 0)/(s > 0, \widetilde{s} > 0)$$

Along this plane, $\mathbf{v}(s, \tilde{s}, \tilde{p}) = \left(-as + b\widetilde{s}, u(as + (c-e)\widetilde{s} - d\widetilde{s}^2), e\widetilde{s}\right)$. Since the third coordinate is positive, the vector points to the interior of the non-negative cone $\mathcal{C}$.

$$II: \ (s = 0)/(\tilde{s} > 0, \widetilde{p} > 0)$$

Along this plane $\mathbf{v}(s, \tilde{s}, \tilde{p}) = \left(b\widetilde{s}, (c-e)\widetilde{s} - d\widetilde{s}^2, e\widetilde{s} + \widetilde{p} - f\widetilde{p}^2\right)$. Since the first coordinate is positive, the vector points to the interior of the non-negative cone $\mathcal{C}$.

$$III: \ (\tilde{s} = 0)/(s > 0, \widetilde{p} > 0)$$

Along this plane $\mathbf{v}(s, \tilde{s}, \tilde{p}) = \left(-as, uas, \widetilde{p} - f\widetilde{p}^2\right)$. Since the second coordinate is positive, the vector points to the interior of the non-negative cone $\mathcal{C}$.

Putting these results together, and invoking the existence and uniqueness theorem for ODE's, it follows that the non-negative cone $\mathcal{C}$ is invariant.

VI. Clinical Implications

It would seem that certain clinical implications are emergent from the model.

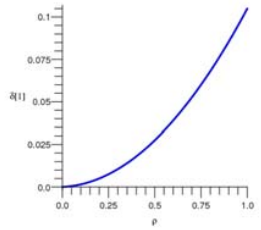

Fig. 7. Graph of $\delta_1(\rho),\ 0 \leq \rho \leq 1$, where δ_1 is the first coordinate of the attractor A in terms of scaled normal and mutant stem cell populations.

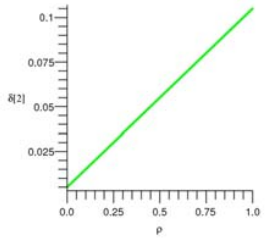

Fig. 8. Graph of $\delta_2(\rho),\ 0 \leq \rho \leq 1$, where δ_2 is the second coordinate of the attractor A in terms of scaled normal and mutant stem cell populations.

(a)When $\rho = 0$, there is no organism response, and the healthy stem cell population would be annihilated.

(b)As ρ increases toward $\rho = 1$, δ_1 (for healthy stem cells) increases at a constant rate toward its maximum

$$\delta_1 = \frac{b(c - e + b)}{da}.$$

(c)As ρ increases toward $\rho = 1$, δ_2 (for mutant stem cells) increases at a constant rate toward its maximum

$$\delta_2 = u\frac{c - e + b}{d}.$$

Note that the equilibrium value δ_2 for the mutant stem cell population also increases with the organism response. This is consistent with the results in [26] , on cancer being a robust system.

One illustrates (a), (b) and (c) using data from Table I. One therefore obtains a parametric curve $A(\delta) = (\delta_1(\rho), \delta_2(\rho)), 0 \leq \rho \leq 1$.

(d)As ρ increases toward $\rho = 1$, δ_3 (mutant progenitor cells) increases toward its maximum

$$\delta_3 = \frac{d + \sqrt{d^2 + 4dfce - 4dfe^2 + 4def\frac{\mu_0}{B\alpha_2}}}{2df}.$$

Observe that $\frac{\partial^2 \delta_3}{\partial \rho^2} < 0$.

(e)It follows that if a therapy is used that enhances the organism response term, then we would expect not only a slower progression, but a smaller equilibrium tumor mass for the avascular stage.

(f) On the other hand, a therapy that reduces or even eliminates the organism response could be expected to reduce the equilibrium value δ_1 below a threshold and would effectively lead to annihilation of the healthy stem cell population.

Mathematical justification is obtained from the following elementary calculations.

(i) For $\rho = 0$, the global attractor is

$$(\delta_1, \delta_2, \delta_3) = \left(0, u\left(\frac{c-e}{d}\right), \frac{d+\sqrt{d^2+4dfce-4dfe^2}}{2df}\right).$$

(ii) For $\rho = 1$, the global attractor is

$$(\delta_1, \delta_2, \delta_3) = \left(\frac{b(c-e+b)}{da}, u\left(\frac{c-e+b}{d}\right), \frac{d+\sqrt{d^2+4dfce-4dfe^2+4defb}}{2df}\right).$$

Next, one looks to how the global attractor changes as a function of the response term ρ. Recall that $b = \frac{\rho\mu_0}{B\alpha_2}$ is the only parameter that depends on ρ. So, for the general case ($\rho \geq 0$), one gets $\frac{\partial\delta_i}{\partial\rho} = \frac{\partial\delta_i}{\partial b}\frac{db}{d\rho} = \frac{\partial\delta_i}{\partial\rho}\left(\frac{b}{\rho}\right)$, for $i = 1, 2, 3$.

(iii) One therefore gets the following inequalities:

$$\frac{\partial\delta_1}{\partial\rho} = \left(\frac{c-e+2b}{da}\right)\left(\frac{\mu_0}{B\alpha_2}\right) > 0,$$

$$\frac{\partial\delta_2}{\partial\rho} = u\left(\frac{c-e}{d}\right)\left(\frac{\mu_0}{B\alpha_2}\right) > 0,$$

$$\frac{\partial\delta_3}{\partial\rho} = \left(\frac{be}{\sqrt{d^2+4dfce-4dfe^2+4dfbe}}\right)\left(\frac{\mu_0}{B\alpha_2}\right) > 0$$

VII. Stability analysis for persistence

The first stage of the analysis is to identify and classify the equilibrium points of the ODE. Recall that

$$\alpha_1 - \mu_1 > 0 \text{ and so } -c+e-b < 0.$$

One will also continue to make regular use of the identifications given in Section V:

$$a = \frac{\mu_0}{\alpha_2},\ b = \frac{\rho\mu_0}{B\alpha_2},\ c = \frac{\alpha_1}{\alpha_2},\ d = \frac{\alpha_{11}}{B\alpha_2},\ e = \frac{\mu_1}{\alpha_2}, f = \frac{\alpha_{22}}{B\alpha_2} \quad (21)$$

The Jacobian matrix for the system (or as it is often called in biological modeling, the variational matrix) is

$$\mathbf{V}(s,\widetilde{s},\widetilde{p}) = \begin{pmatrix} -\frac{\mu_0}{\alpha_2} & \frac{\rho\mu_0}{B\alpha_2} & 0 \\ u\frac{\mu_0}{\alpha_2} & u\left(\frac{\alpha_1}{\alpha_2} - \frac{2\alpha_{11}\widetilde{s}}{B\alpha} - \frac{\mu_1}{\alpha_2}\right) & 0 \\ 0 & \frac{\mu_1}{\alpha_2} & 1-\frac{2\alpha_{22}\widetilde{p}}{B\alpha_2} \end{pmatrix} \quad (22)$$

$$= \begin{pmatrix} -a & b & 0 \\ ua & u(c-2d\tilde{s}-e) & 0 \\ 0 & e & 1-2f\tilde{p} \end{pmatrix} \quad (23)$$

Equilibrium 1: The equilibrium is $(0,0,0)$. Here, the variational matrix is

$$\mathbf{V}(0,0,0) = \begin{pmatrix} -\frac{\mu_0}{\alpha_2} & \frac{\rho\mu_0}{B\alpha_2} & 0 \\ \frac{u\mu_0}{\alpha_2} & u\left(\frac{\alpha_1}{\alpha_2} - \frac{\mu_1}{\alpha_2}\right) & 0 \\ 0 & \frac{\mu_1}{\alpha_2} & 1 \end{pmatrix} \quad (24)$$

$$\begin{pmatrix} -a & b & 0 \\ ua & u(c-e) & 0 \\ 0 & e & 1 \end{pmatrix} \quad (25)$$

There are two positive eigenvalues

$$1 \text{ and } \frac{uc-e-a+\sqrt{u^2c^2-2ceu^2+2auc+u^2e^2-2aeu+a^2+4aub}}{2}, \quad (26)$$

and one negative eigenvalue

$$\frac{uc-e-a-\sqrt{u^2c^2-2ceu^2+2auc+u^2e^2-2aeu+a^2+4aub}}{2} \quad (27)$$

To see that the signs of the eigenvalues are as claimed, observe that the discriminant $c^2-2ceu+2acu+e^2u^2-2aeu+a^2+4abu$ can be written as $(cu-eu+a)^2+4a(cu-a+bu)$. The result follows.

Equilibrium 2: The next equilibrium we treat is $(0,0,1/f)$. The variational matrix at this point is

$$\mathbf{V}(0,0,1/f) = \begin{pmatrix} -\frac{\mu_0}{\alpha_2} & \frac{\rho\mu_0}{B\alpha_2} & 0 \\ \frac{u\mu_0}{\alpha_2} & u\left(\frac{\alpha_1}{\alpha_2} - \frac{\mu_1}{\alpha_2}\right) & 0 \\ 0 & \frac{\mu_1}{\alpha_2} & -1 \end{pmatrix} \quad (28)$$

$$= \begin{pmatrix} -a & b & 0 \\ ua & u(c-e) & 0 \\ 0 & c & -1 \end{pmatrix} \quad (29)$$

There are two negative eigenvalues

$$-1 \text{ and } \frac{uc-ue-a-\sqrt{uc^2-2uce+2auc+u^2e^2-2aeu+a^2+4aub}}{2}, \quad (30)$$

and one positive eigenvalue

$$\frac{uc-ue-a+\sqrt{uc^2-2cue+2auc+u^2e^2-2aeu+a^2+4abu}}{2}.$$

The reasons for the algebraic signs are the same as for the previous argument. It follows that $(0,0,1/f)$ is a saddle point.

Equilibrium 3: The next equilibrium point that we treat is

$$\left(\frac{b(c-e+b)}{da}, u\frac{c-e+b}{d}, \frac{d-\sqrt{d^2+4dfce-4dfe^2+4dfbe}}{2df}\right) \quad (31)$$

The first two coordinates are positive. However, the third coordinate is strictly negative. To see that we rewrite the discriminant

$$d^2 + 4dfce - 4dfe^2 + 4dfbe = d^2 + 4def\,(c - e + b)\,.$$

Therefore the square root is strictly larger than d and it follows that this equilibrium point is not in the positive cone $\mathcal{C}$.

Equilibrium 4: There is only one equilibrium point that is interior to $\mathcal{C}$, namely,

$$(\delta_1, \delta_2, \delta_3) = \left(\frac{b(c-e+b)}{da}, u\left(\frac{c-e+b}{d}\right), \frac{d+\sqrt{d^2+4dfce-4dfe^2+4dfbe}}{2df}\right) \tag{32}$$

The variational matrix at this point is

$$\mathbf{V}(\delta_1, \delta_2, \delta_3) = \begin{pmatrix} -\frac{\mu_0}{\alpha_2} & \frac{\rho\mu_0}{B\alpha_2} & 0 \\ u\frac{\mu_0}{\alpha_2} & u\left(\frac{\alpha_1}{\alpha_2} - \frac{2\alpha_{11}\delta_2}{B\alpha} - \frac{\mu_1}{\alpha_2}\right) & 0 \\ 0 & \frac{\mu_1}{\alpha_2} & 1 - \frac{2\alpha_{22}\delta_3}{B\alpha_2} \end{pmatrix} \tag{33}$$

$$= \begin{pmatrix} -a & b & 0 \\ ua & u(c - 2d\delta_2 - e) & 0 \\ 0 & e & 1 - 2f\delta_3 \end{pmatrix} \tag{34}$$

The eigenvalues are

$$1 - 2f\delta_3 \tag{35}$$

$$uc/2 - ud\delta_2 - ue/2 - a/2 + \frac{\sqrt{u^2c^2 - 4u^2cd\delta_2 - 2u^2ce + 2auc}}{2} \frac{\sqrt{+4d^2\delta_2^2 + 4ud\delta_2 e - 4adu^2\delta_2 + u^2e^2 - 2aeu + a^2 + 4uab}}{2},$$

$$uc/2 - ud\delta_2 - ue/2 - a/2 - \frac{\sqrt{u^2c^2 - 4u^2cd\delta_2 - 2u^2ce + 2acu}}{2} \frac{\sqrt{+4d^2u\delta_2^2 + 4d\delta_2 e - 4u^2ad\delta_2 + e^2 - 2aeu + a^2 + 4aub}}{2}.$$

Note that

$$1 - 2f\delta_3 = 1 - 2f\left(\frac{d+\sqrt{d^2+4dfce-4dfe^2+4dfbe}}{2df}\right)$$
$$= 1 - \left(1 + \frac{\sqrt{d^2+4dfce-4dfe^2+4dfbe}}{d}\right) < 0.$$

For the other eigenvalues, observe that if one writes the discriminant $u^2c^2 - 4u^2cd\delta_2 - 2u^2ce + 2uac + 4u^2d^2\delta_2^2 + 4ud\delta_2 e - 4ad\delta_2 + u^2e^2 - 2uae + a^2 + 4uab$ in terms of

$$(uc/2 - ud\delta_2 - ue/2 - a/2)^2$$

one obtains a quantity of the form $(uc/2 - ud\delta_2 - ue/2 - a/2)^2 - P$, where $P > 0$. Note also that $c/2 - d\delta_2 - e/2 - a/2 < 0$. It follows that the other two eigenvalues are also negative. The equilibrium

$$(\delta_1, \delta_2, \delta_3) = \left(\frac{b(c-e+b)}{da}, u\left(\frac{c-e+b}{d}\right), \frac{d+\sqrt{d^2+4dfce-4dfe^2+4dfbe}}{2df}\right).$$

is therefore a local attractor.

The interior equilibrium $(\delta_1, \delta_2, \delta_3)$ is a global attractor: The unique interior equilibrium is not only a local attractor, but is in fact a global attractor for the non-negative cone. To establish this, one can go back to the ODE (19).

$$\begin{aligned} \frac{ds}{d\zeta} &= -as + b\widetilde{s} \\ \frac{d\widetilde{s}}{d\zeta} &= u\left(as + (c-e)\,\widetilde{s} - d\widetilde{s}^2\right)\,. \\ \frac{d\widetilde{p}}{d\zeta} &= e\widetilde{s} + \widetilde{p} - f\widetilde{p}^2 \end{aligned} \tag{36}$$

Notice that the first two equations are independent of the mutant progeny term $\widetilde{p}$. The approach in this work will therefore be to first analyze the equations for $\frac{ds}{d\zeta}$ and $\frac{d\widetilde{s}}{d\zeta}$; and then use the derived information in the third equation for $\frac{d\widetilde{p}}{d\zeta}$.

The first two equations are

$$\begin{aligned} \frac{ds}{d\zeta} &= -as + b\widetilde{s} \\ \frac{ds}{d\zeta} &= u\left(as + (c-e)\,\widetilde{s} - d\widetilde{s}^2\right)\,. \end{aligned} \tag{37}$$

The non-negative quadrant of the $(s, \tilde{s})$ plane is therefore partitioned by two null-clines η_1 and η_2 given by $s = \frac{b}{a}\tilde{s}$ and $s = \frac{1}{a}\left[d\widetilde{s}^2 - (c-e)\,\widetilde{s}\right]$. There are two equilibrium points, the origin $(0,0)$, and $(\delta_1, \tilde{\delta}_2)$, $(\delta_1, \delta_2$ from Equilibrium 4).

The variational matrix for the system (37) is $\mathbf{J} = \begin{pmatrix} -a & b \\ ua & u(c - 2d\tilde{s} - e) \end{pmatrix}$.

At the origin this becomes $\mathbf{J} = \begin{pmatrix} -a & b \\ ua & u(c - e) \end{pmatrix}$. By standard calculations, this matrix has two non-zero eigenvalues of opposite sign. It follows that the origin is a saddle point.

At the point (δ_1, δ_2) interior to the non-negative quadrant of the $(s, \tilde{s})$ plane, $\mathbf{J} = \begin{pmatrix} -a & b \\ ua & u\,(-(c-e) - 2b) \end{pmatrix}$, which is of the form $\mathbf{J} = \begin{pmatrix} -a & b \\ a & -gu \end{pmatrix}$, where a, b, g are all strictly positive terms. The characteristic equation is then $\chi(x) = x^2 + x\,(a + ug) + aug - ab$. The roots of this equation are

$$x = \frac{-(a+gu) \pm \sqrt{(a+gu)^2 + 4a(gu - b)}}{2}$$

both real and negative.

The nullclines η_1 and η_2 of (37) partition the nonnegative quadrant of the $(s, \tilde{s})$ plane. We again use roman numerals I, II, III, and IV.

Suppose that P_0 is in the interior II^0. The point P_0 belongs to a unique solution trajectory $P(\zeta) = (s(\zeta), \tilde{s}(\zeta))$ of (37).

By standard phase plane analysis (see Figure 1. a.), $\frac{ds}{d\zeta} < 0$ and $\frac{d\tilde{s}}{d\zeta} < 0$ along $P(\zeta)$. Moreover, $s(\zeta)$ and $\tilde{s}(\zeta)$ are both bounded below by δ_1 and δ_2 respectively. It follows that the trajectory $P(\zeta) = (s(\zeta), \tilde{s}(\zeta))$ has a limit point Ω. By the theory of ODE's, $\Omega \neq (0,0)$ must be an equilibrium point for the system. But equation (37) has only two equilibrium points, $(0,0)$ and (δ_1, δ_2). Therefore, $\Omega = (\delta_1, \delta_2)$. A completely similar argument shows that (δ_1, δ_2) is the limit point for any trajectory that begins in the interior of region IV^0.

If $P_0 \neq (\delta_1, \delta_2)$ belongs to any nullcline, then by standard phase plane analysis, the vector field is non-zero, and points into the interior of either II or IV. The flow therefore carries the point into the interior of II or IV respectively and we may then argue as above.

Suppose that P_0 starts in I^0 or III^0. The coordinate functions are monotone. Those decreasing and bounded below or those that increasing are bounded above. There are two possibilities. The flow $P(\zeta) = (s(\zeta), \tilde{s}(\zeta))$ may reach and cross one of the null-clines in finite time. Then argue as above. Or, $P(\zeta) = (s(\zeta), \tilde{s}(\zeta))$ remains interior to I^0 or III^0 respectively. Again, since the coordinate functions are bounded and monotone as just described, the flow has a limit point $\Omega \neq (0,0)$. By uniqueness of the equilibrium point, the limit point Ω is identical with the point (δ_1, δ_2).

For the coordinate axes, note that if $\tilde{s} = 0$, then the vector field is of the form $(-as, as)$ and so points into I^0. By the theory of ODE's, the flow is carried into I^0. Now, argue as above. In the same way, if $s = 0$, the vector field is of the form $\left(b\tilde{s}, u\left((c-e)\tilde{s} - d\tilde{s}^2\right)\right)$, and points into III^0 and by the same reasoning as for the previous case, the flow is carried into III^0. Again, now argue as above.

It follows that (δ_1, δ_2) is a global attractor for the $(s(\zeta), \tilde{s}(\zeta))$ system given by equation (50).

Adverting now to

$$\frac{d\widetilde{p}}{d\zeta} = \frac{\mu_1}{\alpha_2}\widetilde{s} + \widetilde{p} - \frac{1}{B\alpha_2}\alpha_{22}\widetilde{p}^2,$$

the third equation of the ODE given by (31), note that from the above analysis of equation (37) we get that as time increases, $\widetilde{s}$ approaches δ_2. Then, given any $\epsilon > 0$, the $(\zeta, \widetilde{p})$ phase-plane trajectories for the third equation are asymptotically dominated by logistic equations of the form

$$\frac{d\widetilde{p}}{d\zeta} = \frac{\mu_1}{\alpha_2}\delta_2 \pm \epsilon + \widetilde{p} - \frac{1}{B\alpha_2}\alpha_{22}\widetilde{p}^2.$$

It follows that $\widetilde{p}$ converges to the solution of

$$\frac{\mu_1}{\alpha_2}\delta_2 + \widetilde{p} - \frac{1}{B\alpha_2}\alpha_{22}\widetilde{p}^2 = 0,$$

which of course gives the same equilibrium value δ_3 as in the Equilibrium 4.

We conclude that $(\delta_1, \delta_2, \delta_3)$ is a global attractor for the interior of the non-negative cone $\mathcal{C}$ for the full system (36), as claimed.

VIII. Conclusion

The PDE terms are used to include spatial diffusion of cell populations prostate cancer stem cells and progeny of cancer stem cells. The stem cells are stationary in proximal region where they reside. The advection term is included for biased cancer stem cells motion. Then intensity poisson process terms are included in the PDEs. correspond with normally observed spatial expansion of an avascular tumor. The traveling wave solutions, which lead to a derived ODE are investigated. The non-negative cone for the traveling wave system is time invariant is showed. This was important to show that prostate cancer cells are persistent. Then proved that the traveling waves have a unique global attractor. Conclusion comments on clinical implications of the model are made.

Consistent with contemporary perspectives, one thinks that promising avenues for continued research will include the development of heterogeneity models, and more complete and clinically verifiable systems based models. These could include transient amplifying cells, luminal cells, as well as cellular and biochemical response terms in both the organism and the cancerous subsystem. Medical treatment terms could be included in a staged and progressive study. It might also be possible to investigate the development of new organism response models for angiogenesis within a multi-scale systems framework.

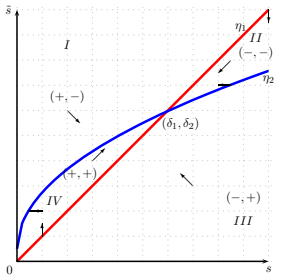

Fig. 1: a: Phase diagram of s and $\tilde{s}$ from system of ODEs .

ACKNOWLEDGMENT

The author would like to thank the Office of Graduate Studies at Middle Tennessee State University for helping support this research project.

REFERENCES

[1] M. Abercrombie, Contact inhibition in tissue. In vitro 6, 128-140, 1970.
[2] R. Agami, All Roads Lead toIKKϵ, Cell 129, 1043-1045, 2007.
[3] Anderson Cancer Center, University of Texas, 2008. Drug therapy to bolster immune system cells found effective toward childhood cancer. Article on work of Lee, D. (Ph.D.), Science Daily, May, 2008.
[4] M. Bertsch, M. E. Gurtin, D. Hilhorst, L. S. Peletier, On interacting populations that disperse to avoid crowding: perservation of segregation, 1985
[5] J. Canosa, On a nonlinear diffusion equation describing population growth. IBM J. Res. Dev. 17, 307-313, 1973.
[6] L. G. Charles, C. X. Yilin, , N. P. Restifo, B. Roessler, M. G. Sanda, Antitumor efficacy of tumor-antigen-encoding recombinant poxvirus immunization in Dunning rat prostate cancer: implications for clinical genetic vaccine development. World Journal of Urology, April, 18 (2), 136-142, 2000.
[7] T. C. Collins, N. J. Maitland, Prostate cancer stem cells. European J. of Cancer 42, 1213-1218, 2006.
[8] E. Conway, D. Huff, J. Smoller, Large time behavior of solutions of systems of nonlinear reaction-diffusion equations. SIAM J. Appl. Math., 35 (1), July, 1-16, 1978.
[9] F. F. Costa K. Le Blanc, B. Brodin, Cancer/Testis antigens, stem cells and cancer. Stem Cells 12(2), 398-404, 2006.
[10] D. Dingli, F. Michor, Successful therapy must eradicate cancer stem cells. Stem Cells 24, 2603-2610, 2006.
[11] G. P. Dunn, et al., The three Es of cancer immunoediting. Annu. Rev. Immunol. 22, 329360, 2004.
[12] M. Fasso, R. Waitz, H. Yafei, R. Tae, N. M. Greenberg, N. Shastri, L. Fong, J. P. Allison, SPAS-1 (stimulator of prostatic adenocarcinoma-specific T cells)/SH3GLB2: A prostate tumor antigen identified by CTLA-4 blockade. Proceedings of the National Academy of Sciences of the United States of America (0027-8424). 105(9), 3509-3514, 2008.
[13] R. A. Fisher, The wave of advance of advantageneous genes. Ann. Eugenics 7, 353-369, 1937.
[14] R. Ganguly, and I. K. Puri, Mathematical model for the cancer stem cell hypothesis. Cell Proliferation 39, 3-14, 2006.
[15] A. L. Garner, Y. Y. Lau, S. W. Jordan, M. D. Uhler, R. M. Gilgenbach, Implications of a simple mathematical model to cancer cell population dynamics. Cell Prolif., 39, 15-28, 2006.
[16] S. Gakkhar, S. Brahampal, R. K. Naji, Dynamical behavior of two predators competing over a single prey. Biosystems, 90, 808-817, 2007.
[17] M. C. Garnick, M. C. Fair, Combating Prostate Cancer. Scientific American 279(6), 74-83, 1998.
[18] M. C. Gong., J. B. Latouche, A. Krause, W. D. W. Heston, N. H. Bander, M. Sadelain, Cancer patient T cells genetically targeted to prostate-specific membrane antigen specifically lyse prostate cancer cells and release cytokines in response to prostate-specific membrane antigen. Neoplasia, 1(2), June. 123-127, 1999.
[19] M. Greaves, M., 2000. Cancer: The Evolutionary Legancy, Oxford University Press.
[20] L. Han, A. Publiese, Epidemics in two competing species. Nonlinear Analysis: Real World Applications, 10(2), 723-744, 2009.
[21] A. L. Harzstark, E. J. Small, Immunotherapy for prostate cancer using antigen-loaded antigen-presenting cells: APC8015 (provenge). Expert Opinion on Biological Therapy, August, 7(8), 1275-1280, 2007.
[22] M. Jakobisiak, et al. Natural mechanisms protecting against cancer. Immunol. Lett. 90, 103122, 2003.
[23] B. T. Kawasaki, and W. L. Farrar Cancer stem cells, CD200 and immunoevasion, Trends in Immunology, 29(10), Issue 10, 464-468, 2008.
[24] E. F. Keller, L. A. Segel, Model for chemotaxis. J. Theor. Biol. 30, 225-234, 1971.
[25] Y. Kiniwa, Y. Miyahara, H. Y. Wang, W. Peng, G. Peng, T.M. Wheeler, T. C. Thompson, J. Lloyd, CD8+ Foxp3+ T cells mediate immunosuppression in prostate cancer. Clinical Cancer Research, December 1(13), 6947-6958, 2007.
[26] H. Kitano, Cancer therapy as a robust system: implications for anti-cancer therapy, Nature Reviews - Cancer, 4, 227-235, 2004.
[27] J. L. Lao, and D. T. Kamei, Investigation of cellular movement in the prostate epithelium using an Agent-based model, J. Theor. biol. 250, 642-654, 2008.
[28] C. Lee, J. A. Sensibar, S. M. Dudek, R. A. Hiipakka, S. T. Liao, Prostatic ductal system in rats: regional variation in morphological and functional activities. Biol. Reprod. 43, 10791086, 1990.
[29] I. C. Mackenzie, Stem cell properties and epithelial malignancies European Journal of Cancer. 42(9), 1204-1212, 2006.
[30] N. J. Maitland, A. T. Collins, prostate cancer stem cells: new therapeutic targets? European Journal of Cancer Supplements, 5(4), 2007.
[31] J. Michalowski, Common molecule notifies immune system of prostate cancer. www.eurekalert.org, Publication release, January 10, 2008.
[32] F. Michor, M. A. Nowak, S. A. Frank, Y. Iwasa, Stochastic elimination of cancer cells. Proc. R. Soc. Lond. B 270, 2017-2024, 2003.
[33] S. J. Morrison, A. C. Spradling, Stem Cells and Niches: Mechanisms that promote stem cell maintenance throughout life, Cell 132, 598-611, 2008.
[34] D. Mukherjee, Uniform persistence in a generalized prey-predator system with parasitic infection. Biosystems, 47, 149-155, 1998.
[35] J. A. Nemeth, C. Lee, Prostatic ductal system in rats: regional variation in stromal organization. Prostate 28, 124128, 1996.
[36] P. C. Nowell, The clonal expansion of tumor cell populations. Science 194, 23-28, 1996.
[37] B. I. Rini., V. Weinberg, L. Fong, S. Conry, R. M. Hershberg, E. J. Small, Combination immunotherapy with prostatic acid phosphatase pulsed antigen-presenting cells (provenge) plus bevacizumab in patients with serologic progression of prostate cancer after definitive local therapy. Cancer, July, 107(1), 67-74, 2006.
[38] M. Rouleau, J. Leger, M. Tenniswood, M., 1990. Ductal heterogeneity of cytokeratins, gene expression, and cell death in the rat ventral prostate. Mol. Endocrinol. 4, 20032013, 1990.
[39] Savage, P., Vosseller, K., Kang, C., Larimore, K., Riedel, E., Wojnoonski, K., Jungbluth, A.A., Allison, J.P., 2008. Recognition of a ubiquitous self antigen by prostate cancer infiltrating CD8+ T lymphocytes. Science, January 319 (5860), 215- 220.
[40] J. A. Schalken, G. Van Leenders, Cellular and molecular biology of the prostate: stem cell biology, Urology, November 62(Supplement 5A), 11-20, 2003.
[41] Schreiber, H. and Rowley, D.A., Mutations in cancer cells can give rise to tumor-specific antigens, but abnormal processing of normal molecules in these cells can also elicit an immune response. Science 319 (5860), 164-165, 2008.
[42] J. A. Sherratt, Wave front propagation in a competition equation with a new motility term modeling contact inhibition between cell populations. Proc. R. Soc. Lond. A 456, 2365-2387, 2000.
[43] J. A. Sherratt, M. A. J. Chaplain, A new mathematical model for avascular tumour growth. J. Math. Biol. 43, 291-312, 2001.
[44] T. Quinn, and Z. Sinkala, Dynamics of prostate cancer stem cells with diffusion and organism response, Biosystems, 96(1), 69-79, 2009.
[45] T. L. Soon, A. K. Cheng, A numerical simulation of avascular tumour growth. Anziam. J. 46, 902-917, 2005.
[46] Y. Sugimura, G. R. Cunha, A. A. Donjacour, Morphogenesis of ductal networks in the mouse prostate. Biol. Reprod. 34, 961971, 1986.
[47] A. R. Uzgare, J. T. Isaacs, Prostate cancer: potential targets of anti-proliferating and apoptotic signaling pathways, International J. of Biochemistry and Cell Biology, 37, 707-714, 2005.
[48] D. Wodarz, N. Komarov, Computational Biology of Cancer. World Scientific Publishing Co. Pte. Ltd., Singapore, 2005.
[49] G. Wang, B. Kovalenko, E. L. Wilson, and D. Moscatelli, Vascular Density is Highest in the Proximal Region of the Mouse Prostate. Prostate. 67(9): 968975, 2007
[50] X. Zang, T. Houston, H. A. Al-Ahmadie, A. M. Serio, V. E. Reuter, J. A. Eastham, P. T. Scardino, P. Sharma, J. P. Allison, B7-H3 and B7x are highly expressed in human prostate cancer and associated with disease spread and poor outcome. PNAS, Biological Sciences/Immunology, December, 104(49), 19458-19463, 2007.